J. Fluid Mech. (1984), *vol.* 144, *pp.* 177–190
Printed in Great Britain

On the formation of ripples on an erodible bed

By B. MUTLU SUMER† AND MEHMET BAKIOGLU
Technical University of Istanbul, Faculty of Civil Engineering, Taskisla, Taksim, Istanbul, Turkey

(Received 23 May 1983 and in revised form 17 January 1984)

A linear stability analysis is presented of both hydraulically smooth and transitional flows over an erodible bed. The present theory is developed to account for the formation of ripples. It is essentially an extension of the theory of Richards (1980) to include the effect of viscosity upon the bed wave stability. The theory takes into consideration that the formation of ripples does not depend on flow depths, and that only the bed-load transport is involved in the formation of ripples. The effect of gravity is included in the analysis through the local inclination of the wavy bed surface. The results show that the bed is unstable (i.e. ripples exist) when the grain Reynolds number is less than a certain value. The limiting values of the grain Reynolds number for ripple existence obtained through present analysis are found to be in good agreement with observations.

1. Introduction

Prediction of flow over an erodible bed covered by bed waves is one of the most significant problems in hydraulic engineering. The flow depends on the bed form, while the bed form depends on the flow: there exists a complex feedback mechanism between the two. More accurate predictions of flow over erodible beds therefore depend on more accurate information on the mechanics of bed form. Ripples are one of the most encountered bed forms and therefore deserve special attention. The problem of the initiation and development of ripples has not been solved in a generally accepted manner, and there are various theories trying to explain the formation of these bed waves. Richards (1980) broadly divided these theories into stability theories and theories involving the propagation of ripples downstream from an initial disturbance. A detailed account of these theories has been given in Richards (1980).

For a comprehensive review of the subject the reader is referred to any one of the excellent review papers by Reynolds (1976), Kennedy (1980) and Engelund & Fredsøe (1982).

Richards (1980) presented a stability theory to account for the occurrence of ripples and dunes. The theory proposed by Richards successfully predicts the occurrence of two separate modes of instability, with wavelengths related to the roughness of the bed and the depth of the flow. It postulates that the former mode corresponds to the formation of ripples and the latter to that of dunes. It should be noted that, in the aforementioned theory, the bed is assumed to be hydraulically rough.

Engelund & Fredsøe (1982), in their review paper, suggest that it would be of interest to carry out an analysis similar to that of Richards for hydraulically smooth bed, pointing out that ripples are usually associated with a smooth bed. In fact, Mantz

† Present address: Technical University of Denmark, Institute of Hydrodynamic and Hydraulic Engineering, 2800 Lyngby, Denmark.

(1978) observed that ripples developed for grain Reynolds number $du_*/\nu \sim 0.1$, which clearly indicates that the bed in his experiments behaved as a hydraulically smooth boundary (here d is the grain size, u_* the shear velocity and ν the kinematic viscosity). On the other hand, some observations show that ripples can be observed up to the values of grain Reynolds number of 20–30 (see figure 6), which suggests that ripples are associated not only with a hydraulically smooth bed but also with a transitional bed.

Quite recently, Hayashi & Onishi (1983) have presented a bed-form stability analysis with the aim of developing a unified theory that will cover the entire range of sand waves from ripples to antidunes. The theory appears to predict three different groups of dominant wavelengths corresponding to ripples, dunes and antidunes. However, as far as the ripple formation is concerned, their results suffer from the fact that the theory does not take into consideration the fact that ripples are associated with hydraulically smooth and transitional beds.

In an earlier study, the authors (Sumer, Bakioglu & Bulutoglu 1982) made an attempt to work out a linear stability analysis for the smooth bed case to explain the occurrence of ripples observed by Mantz; and indeed the stability analysis predicted the occurrence of bed instability, giving the preferred initial length of bed waves to be proportional to the viscous lengthscale ν/u_*.

The present paper presents a linear stability theory of a plane erodible bed to account for the occurrence of ripples in a more general case.† The theory takes into consideration the following facts, which are the reported features of ripple formation: (*a*) the bed usually behaves as a transitional boundary but it may also behave as a hydraulically smooth one if the grain Reynolds number is sufficiently small; (*b*) the formation of ripples does not depend on flow depths; (*c*) only the bed-load transport of sediment is involved in ripple formation; and (*d*) gravitational force is important, as it impedes grain motion up stoss slopes and aids it down lee slopes. The 'stability' part of the present theory, including the sediment analysis, follows the line of Richards (1980). Although the flow model adopted here is different from that of Richards, the present theory is principally an extension of that of Richards to include the viscous lengthscale ν/u_* by assuming flow over smooth and transitional boundaries. The result is that the bed is unstable (i.e. ripples will exist) when the grain Reynolds number du_*/ν is less than a certain value.

In §2 the flow over a small-amplitude wavy bed is analysed. By relating the sediment transport to the wall shear stress obtained through the flow analysis, the stability of the bed wave is examined in §3. The results are presented and discussed in §4.

2. Flow over a small-amplitude wavy bed

Suppose a plane erodible bed is slightly perturbed so that the bed displacement is given by

$$h = a\,\mathrm{e}^{\mathrm{i}(kx-\sigma t)}, \tag{1}$$

where a is the amplitude, k is the wavenumber of the bed and σ its growth rate. In order to determine whether the bed is stable, it is necessary to reveal the character of the flow past the bed having small perturbations and to associate it with the transport of sediment. In fact, the latter information, along with the continuity equation of sediment transport, will enable us to determine the evolution of the perturbed bed.

† Earlier results of this study have been presented at the Second International Symposium on River Sedimentation held in Nanjing, China (Sumer & Bakioglu 1983).

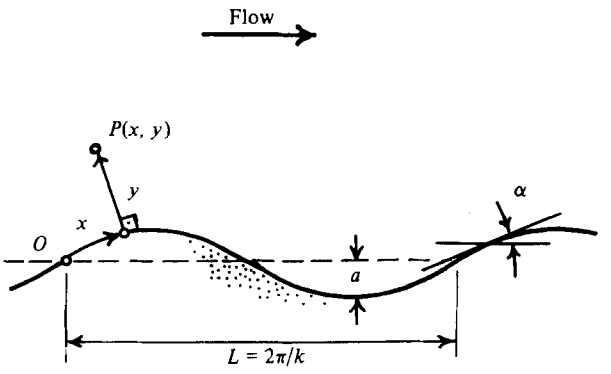

FIGURE 1. Definition sketch.

We assume that the time scale of the flow development over the bed form is small compared with that of the bed-form development.† The latter suggests that the flow over the perturbed bed can be assumed to be steady at times that are short compared with the development time of the bed form. Therefore we consider a steady flow over a small-amplitude solid wavy boundary. Since the formation of ripples does not depend on flow depths (see §1), we further consider the flow to take place in the half-space $y > 0$, where y is the distance from the boundary.

Thomas Hanratty and his group at the University of Illinois (Zilker, Cook & Hanratty 1977; Thorsness, Morrisroe & Hanratty 1978) have carried out a series of experiments on shear-stress distributions in flows over solid wavy walls. They have also developed and convincingly verified a linearized model for smooth, wavy-boundary flow. Their model appears to be applicable for all bed-form amplitudes smaller than those creating flow separation. A detailed account of the model is given in Thorsness *et al.* (1978), while Zilker *et al.* (1977) present the results of the experiments.

It is the model of Thorsness *et al.* that the present study adopts to determine the steady flow over a small-amplitude wavy wall. In this study this model is extended to include also the case when the wall falls into the transitional-boundary category; this is because ripples are associated not only with a smooth bed but also with a transitional bed (see §1). For convenience, the Thorsness *et al.* theory, along with the present extension, will be summarized here very briefly.

We use the boundary-layer coordinate system shown in figure 1. The linearized metrical coefficients of this coordinate system are

$$h_x = 1 + ak^2 y\, e^{ikx}, \quad h_y = 1. \tag{2}$$

For convenience, in the preceding equation and (only) throughout this section, lengths are made dimensionless with respect to the ratio ν/u_* of the kinematic viscosity to the shear velocity, and velocities are made dimensionless with respect to the shear velocity $u_* = (\bar{\tau}_w/\rho)^{\frac{1}{2}}$ (where $\bar{\tau}_w$ is the unperturbed wall shear stress).

The stream function, defined by

$$u = \frac{1}{h_y}\frac{\partial \psi}{\partial y} = \frac{\partial \psi}{\partial y}, \quad v = -\frac{1}{h_x}\frac{\partial \psi}{\partial x}, \tag{3}$$

is written as

$$\psi = \int_0^y \bar{U}(y)\, dy + aF(y)\, e^{ikx}, \tag{4}$$

† The validity of this assumption can be readily seen from Richards' (1980) calculations.

where u and v are the velocity components in the x- and y-directions respectively and $\bar{U}$ is the unperturbed velocity distribution. The first term on the right-hand side of (4) corresponds to the unperturbed flow and the last term to the wave-induced flow.

Substituting (4) into the vorticity equation gives (to the first order in a) the following equation for F:

$$ik[\bar{U}(F''-k^2F)-\bar{U}''F+k^2\bar{U}^2] = F^{IV}-2k^2F''+k^4F+2k^2\bar{U}''-k^4\bar{U}+R, \tag{5}$$

where

$$R = ik^3\bar{r}_{xx}-ik^3\bar{r}_{yy}+3k^2\bar{r}'_{xy}+ik(\hat{r}'_{xx}-\hat{r}'_{yy})+k^2\hat{r}_{xy}+\hat{r}''_{xy}. \tag{6}$$

Here $r_{ij} = \bar{r}_{ij}+a\hat{r}_{ij}e^{ikx}$, in which $\bar{r}_{ij}$ is the unperturbed Reynolds stress and $a\hat{r}_{ij}e^{ikx}$ the wave-induced part.

The boundary conditions are

$$F = 0, \quad F' = 0 \quad \text{at} \quad y = 0, \tag{7}$$

$$F = \bar{U}, \quad F' = \bar{U}' \quad \text{at} \quad \text{large } y. \tag{8}$$

The wall shear stress τ_w and the wall pressure p_w can be obtained from the solution of (5), subject to the boundary conditions in (7) and (8), since at $y = 0$

$$\tau_w = \bar{\tau}_w+aF''(0)e^{ikx}, \tag{9}$$

$$p_w = -\frac{ia}{k}[F'''(0)+k^2\bar{U}'(0)]e^{ikx}. \tag{10}$$

The calculation of the wave-induced flow depends on how the Reynolds stress is modelled. Thorsness *et al.* (1978) found an approach used by Loyd, Moffat & Kays (1970) to be useful for this purpose. Loyd *et al.* neglected the effect of the normal Reynolds stresses and used an eddy-viscosity concept to model r_{xy}:

$$r_{xy} = \frac{\nu_T}{\nu}(2e_{xy}), \tag{11}$$

$$\frac{\nu_T}{\nu} = l_m^2|2e_{xy}|, \tag{12}$$

where ν_T is the eddy viscosity and e_{xy} the xy-component of the rate-of-strain tensor, which is given by

$$2e_{xy} = \bar{U}'+a(k^2F-k^2\bar{U}+F'')e^{ikx}. \tag{13}$$

Furthermore, they adopted the van Driest equation for the mixing length l_m:

$$l_m = \kappa y[1-\exp(-y\tau_w^{\frac{1}{2}}/A)], \tag{14}$$

where κ is the von Kármán constant and A the van Driest damping factor, which, in the present context, is given by

$$A = \bar{A}+\frac{ak_1\bar{A}ik\hat{p}_w}{1+ikk_{LP}}e^{ikx}. \tag{15}$$

Here $\bar{A}$ is the unperturbed value of A; k_1 is a parameter representing the influence of the pressure gradient on A, the pressure gradient being caused by the wavy geometry of the bed; and k_{LP} is another parameter introducing the fact that the response of A to the wall quantities is not instantaneous.

In the present study, the expression for ν_T is modified to represent the influence

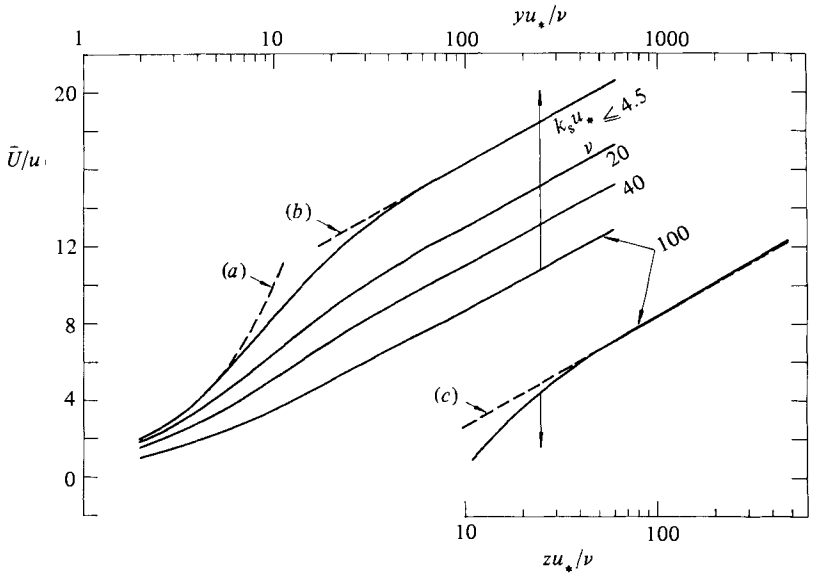

FIGURE 2. Unperturbed velocity distributions obtained through (18). κ was taken as 0.41 and $\bar{A}$ as 25. (*a*) $\bar{U}/u_* = yu_*/\nu$, velocity distribution in the viscous sublayer when the boundary is hydraulically smooth; (*b*) $\bar{U}/u_* = (1/\kappa)\ln(yu_*/\nu)+5.1$, that in the logarithmic layer when the boundary is hydraulically smooth; (*c*) $\bar{U}/u_* = (1/\kappa)\ln(30\,z/k_s)$, that in the logarithmic layer when the boundary is completely rough, in which $z = y+\Delta y$.

of surface roughness as far as the transitional-boundary case is concerned. Following Cebeci & Chang (1978), we rewrite l_m in (14) as

$$l_m = \kappa(y+\Delta y)\{1-\exp[-(y+\Delta y)\tau_w^{\frac{1}{2}}/A]\}. \tag{16}$$

This expression is based on Rotta's (1962) model, which recognizes that the velocity profiles for smooth and rough walls can be similar, provided that the coordinates are displaced. Cebeci & Chang give the coordinate displacement Δy as

$$\Delta y = 0.9[k_s^{\frac{1}{2}} - k_s \exp(-\tfrac{1}{6}k_s)], \tag{17}$$

which relates Δy to the Nikuradse equivalent sand roughness k_s of the wall. Cebeci & Chang report that the expression in (17) is valid for $4.535 < k_s < 2000$, with the lower limit corresponding to the upper bound for a hydraulically smooth boundary.

For the calculations, a van Driest mixing-length equation was used to calculate the unperturbed velocity distribution

$$\bar{U} = 2\int_0^y \frac{dy}{1+\left\{1+4\kappa^2(y+\Delta y)^2\left[1-\exp\left(-\frac{y+\Delta y}{\bar{A}}\right)\right]^2\right\}^{\frac{1}{2}}}. \tag{18}$$

Although this expression is a rather cumbersome one, its utilization with the aid of simple numerical integration techniques does not lead to any objectionable time loss. The velocity distributions obtained through (18) are illustrated in figure 2 for various values of $k_s u_*/\nu$. As seen from the figure: (*a*) $\bar{U}$ tends to the linear distribution $\bar{U} = y$ for small values of y and to the logarithmic distribution $\bar{U} = (1/\kappa)\ln y + 5.1$ for large values of y for hydraulically smooth beds; and (*b*) it tends to the logarithmic

distribution $\overline{U} = (1/\kappa) \ln (30\ z/k_s)$ for large values of y for rough beds in which $z = y + \Delta y$ (Monin & Yaglom 1971).

Other input quantities for the calculations are κ, $\overline{A}$, k_1 and k_{LP}. The von Kármán constant κ was taken as 0.41. As to the van Driest damping factor $\overline{A}$, Cebeci & Chang (1978) report that the available experimental data (k_s ranging from 20 to about 2000) compare favourably well with their calculations in which they introduce the influence of wall roughness through the quantity Δy, keeping the van Driest damping factor constant, irrespective of the wall roughness. Following Cebeci & Chang, the unperturbed damping factor $\overline{A}$ was kept constant throughout the calculations, taking the usual value $\overline{A} = 25$. As far as the parameters k_1 and k_{LP} are concerned, they are introduced in the analysis, as they enable us to handle the damping factor A in the case of a wavy boundary. Hence it appears that they should have no dependence upon the category of the wall. So, for the calculations, the values of these parameters can be taken as those recommended for smooth walls. Thorsness *et al.* (1978) give a detailed account of the influence of these parameters on the final results. On the basis of comparison of their results (with various combinations of k_1 and k_{LP}) with the available data, they recommend $k_1 = -60$ and $k_{LP} = 3000$ (see also Zilker *et al.* 1977). The latter values were employed for the present calculations, irrespective of the boundary roughness. The fact that the present results tend to that of Richards' (1980) rough model (see §4) as k_s approaches the upper bound for transitional boundary reveals the validity of our assumption that the values of k_1 and k_{LP} recommended for smooth walls can be used equally well for rough boundaries.

Numerical solutions to (5) were obtained through a finite-difference technique. The fourth-order differential equation and also the boundary conditions are approximated by finite-difference equations, so that derivatives are expressed up to fifth- or sixth-order central differences at pivotal points. Also difference correction terms, beginning with fifth- or sixth-order central differences, were taken into account to improve the solution (Fox 1957).

3. Sediment transport and stability analysis

3.1. *Sediment transport formula*

In the present context, we consider the sediment transport as bed load, neglecting any suspended load on the ground that only the bed-load transport mode is involved in ripple formation (see §1). We adopt Bagnold's (1956) bed-load formula for this purpose. It relates the rate of work done in moving the bed load along the bed against total resistance to the available energy in the flow where the bed-load transport takes place. This gives

$$q_b = \frac{Be_b}{(s-1)\, g\rho^{\frac{1}{2}}} \frac{(\tau_w - \tau_{cr})\, \tau_w^{\frac{1}{2}}}{(c \tan\phi + \tan\alpha)\cos a}, \tag{19}$$

where q_b is the bed-load discharge, α the local inclination of the perturbed bed surface to the horizontal, ϕ the friction angle, e_b an efficiency factor of order 0.1, s the specific gravity of grains, g the acceleration due to gravity and τ_{cr} the critical shear stress. The coefficient B in (19) is a function of grain Reynolds number, which tends asymptotically towards the value 8.5 as the grain Reynolds number increases (Yalin, 1972, p. 119). However, the explicit form of this function is not needed for the present purpose.

The factor c in (19) does not appear in the original work of Bagnold. The necessity for its introduction, as well as the discussion of its magnitude, is clarified below.

By definition, the bed-load motion takes place in the so-called bed layer immediately above the bed, and the thickness ϵ of the bed layer is proportional to the grain size: $\epsilon \sim d$. For a bed of local inclination α, the resisting force opposing the bed-load motion is the sum of (*a*) the gravity force, (*b*) the friction force and (*c*) other resisting forces which are of minor importance. Let C_b denote the bed concentration by weight. The gravity-induced resisting force per unit area of the bed is then $C_b \epsilon \sin\alpha$. As to the friction force, it is provided by the normal forces exerted by the bed-load particles across a surface of the non-moving bed. However, some of the bed-load particles move in short jumps. This, on the average, will cause the normal load on the non-moving bed to be reduced: this means that an average reduction in the friction force should be expected. Thus the normal force per unit area of the bed surface is $cC_b \epsilon \cos\alpha$ and then the friction force is $cC_b \epsilon \cos\alpha \tan\phi$, where the factor c is included to compensate for the latter effect. This factor would be unity if there was no 'jumping' mode in the bed-load transport, while it would tend to zero if all the particles of the bed load were in 'jumping' mode. Therefore c should be in the range $0 < c < 1$. To provide an estimate for c, we can assume that the friction force generated by the bed-load particles which are in contact with the non-moving bed surface can be expressed as $C_b d \cos\alpha \tan\phi$. Considering that the proportionality ϵ/d is approximately equal to 2, it follows that $c \approx 0.5$. Although, owing to the possible interaction between particles moving in contact with the bed and those in 'jumping' mode, the friction force can be expected to be a little higher than $C_b d \cos\alpha \tan\phi$, and thus the value of c should be correspondingly larger than 0.5, these possible deviations should not be significant, and therefore are not considered in the present analysis.

As has been mentioned in §1, gravitational force is important in ripple formation. In this connection, one should note that Bagnold's formula in its present form (19) takes into account the effect of gravitational force through the local inclination of the bed.

3.2. *Stability analysis*

The sediment continuity equation is

$$\frac{\partial q_b}{\partial x} = -(1-n)\frac{\partial h}{\partial t}, \tag{20}$$

where n is the porosity of the bed. Substituting (1) and the linearized form of (19) into (20), we obtain, to first order in a,

$$\sigma = \frac{Be_b\beta}{(s-1)(1-n)g\rho^{\frac{3}{2}}} \frac{3\bar{\tau}_w - \tau_{cr}}{2} \bar{\tau}_w^{\frac{1}{2}} k\left(\frac{\tilde{\tau}_w/\bar{\tau}_w}{a} - \beta k\mathrm{i}\right), \tag{21}$$

where $\tilde{\tau}_w$ is the wave-induced part of the wall shear stress defined by

$$\tau_w = \bar{\tau}_w + \tilde{\tau}_w e^{\mathrm{i}kx} \tag{22}$$

and β is

$$\beta = \frac{1}{c\tan\phi}. \tag{23}$$

The bed is unstable when $\sigma_i > 0$. Here σ_i is the imaginary part of σ.

4. Results and discussions

Since the numerical technique of the present study differs from that of Thorsness *et al.* (1978), the present numerical technique was tested against theirs by comparing the smooth-boundary results of the present study with the corresponding results in

Thorsness *et al.* As we are interested in the stability of the bed and thus in the wall shear stress (21), the wall shear stress calculated through the present technique was compared with that of Thorsness *et al.*, and a good agreement was observed (for further details see Sumer *et al.* 1982). As far as the formation of ripples is concerned, one of the most significant results associated with the wall shear stress is that it appears to follow the bed perturbation with a phase lag ranging from 25° to 80° for the wavenumber range of interest of the present study (i.e. for $0.001 < k\nu/u_* < 0.1$), the phase lag decreasing with increasing $k\nu/u_*$ (see Thorsness *et al.* 1978). As to the phase lag, although a direct comparison is not possible, the latter findings appear to be in qualitative agreement with Richards' (1980) relevant results, where the stress maximum was found to be upstream of the crest of the small perturbation to the bed.

With regards to the case of the bed behaving as a transitional boundary, our calculations show that the amplitude of the wave-induced part of the wall shear stress somewhat decreases with increasing roughness, the phase lag increasing only slightly. For example, for $k\nu/u_* = 0.02$, the non-dimensionalized amplitude $|\tilde{\tau}_w|/(\bar{\tau}_w a u_*/\nu)$ decreases from 0.185 to 0.115 while the phase lag increases from 39° to 43° as the bed changes from a smooth to a rough wall with $k_s u_*/\nu = 30$. Although no clear explanation is found for the slight increase in phase lag, the decrease in amplitude can be explained as follows. In the case of the smooth wall the perturbation in wall shear stress is induced by the wavy geometry of the wall; whereas in the case of the rough wall there is an additional effect which actually counteracts that due to the wall geometry. This new effect is caused by the wall roughness: the cross-currents in the boundary layer are enhanced by the vortex shedding caused by the presence of the roughness elements; therefore the fast-moving fluid in the outer layers are carried into the neighbourhood of the wall in larger quantities than in the case of the smooth wall. This makes the near-wall flow in the rough-boundary case feel the waviness of the wall less than in the case of smooth wall. The latter implies that the amplitude of the wave-induced part of the wall shear stress should decrease with increasing roughness.

To facilitate comparison with Richards's (1980) rough-model results, the imaginary part of the wave-induced wall shear stress $\tilde{\tau}_{wi}$ is plotted in the form of $(\tilde{\tau}_{wi}/\bar{\tau}_w)/ak$ against the roughness Reynolds number $k_s u_*/\nu$ for various values of kk_s in figure 3. In this figure the results of Richards' work are also plotted, taking the roughness length z_0 in his model to be $\frac{1}{30}k_s$ (Monin & Yaglom 1971, p. 289). As seen from the figure, the present results tend to Richards's at $k_s u_*/\nu = 65$–70. This result has the following two implications. First, the transitional-boundary results of the present study tend to the rough case at the correct value of $k_s u_*/\nu$ ($= 65$–70), which is the upper bound for transitional boundary, and secondly, the rough-boundary results of the present work appear to be in good agreement with Richards' corresponding findings. From dimensional considerations it is easy to show that, for a specified value of kk_s, $(\tilde{\tau}_{wi}/\bar{\tau}_w)/ak$ should be a constant times $k_s u_*/\nu$ when $k_s u_*/\nu < 4.5$, and it should tend to a constant when $k_s u_*/\nu > 70$. It should be noted that the results presented in figure 3 appear to reveal this behaviour.

As stated in §3.2, the bed is unstable when the imaginary part of growth rate σ is positive. From (21) the growth rate of bed perturbation is proportional to

$$\omega = \frac{k\nu}{u_*}\left[\frac{\tilde{\tau}_{wi}}{\bar{\tau}_w a u_*/\nu} - \frac{\beta k\nu}{u_*}\right].$$

The results showed that, for $\beta = 0$, the growth rate increases monotonically with $k\nu/u_*$, and thus the bed is always unstable, in agreement with Richards's (1980)

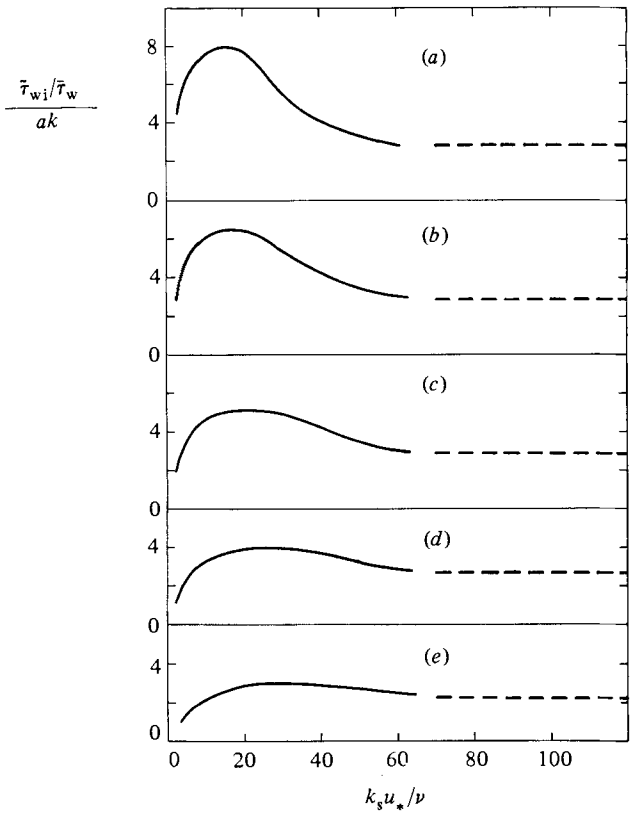

FIGURE 3. Imaginary part of the wave-induced wall shear stress plotted against the roughness Reynolds number $k_s u_*/\nu$. ---, Richards's (1980) solution for rough bed. (*a*) $kk_s = 0.08$; (*b*) 0.15; (*c*) 0.3; (*d*) 0.6; (*e*) 1.2.

corresponding result. (Note that, from (19), it can be readily seen that $\beta = 0$ corresponds to that case when the gravity effect is not taken into consideration.) The results for varying $k_s u_*/\nu$ are shown in figure 4, where β is taken as 3.2, which can be considered as an average value for that parameter, and $c = 0.5$ and $\tan\phi = 0.63$ (an average value for $\tan\phi$; Bagnold 1973). Figure 5 shows the stability diagram from the results plotted in figure 4. As seen from figure 5, there exists an upper limit to the existence of instability of the bed; this upper limit is $k_s u_*/\nu = 58.5$. Since, in the present study, the instability of the bed is associated with the occurrence of ripples, it can be concluded that above $k_s u_*/\nu = 58.5$, no ripples will exist.

For flow above a bed where sediment grains are in motion, the problem of how to determine the Nikuradse equivalent sand roughness has not been solved in a generally accepted manner. Engelund & Hansen (1967, p. 39) report that an analysis they carried out for flows of plane bed (but with sediment in motion) indicated a value of $k_s = 2.5\,d$ on average. Becchi (1983) reproduces the presently available data on the Darcy–Weisbach friction coefficient f for sediment carrying flows with plane beds, where $(8/f)^{\frac{1}{2}} - 2.5 \ln (R/d)$ has been plotted as a function of two parameters, namely the grain Reynolds number du_*/ν and a parameter which can easily be converted to the Shields parameter $u_*^2/g(s-1)d$. Here R is the hydraulic radius. A plot of the data $(8/f)^{\frac{1}{2}} - 2.5 \ln (R/d)$ versus du_*/ν for specified values of Shields parameter has indeed revealed that the Nikuradse equivalent sand roughness can be taken as

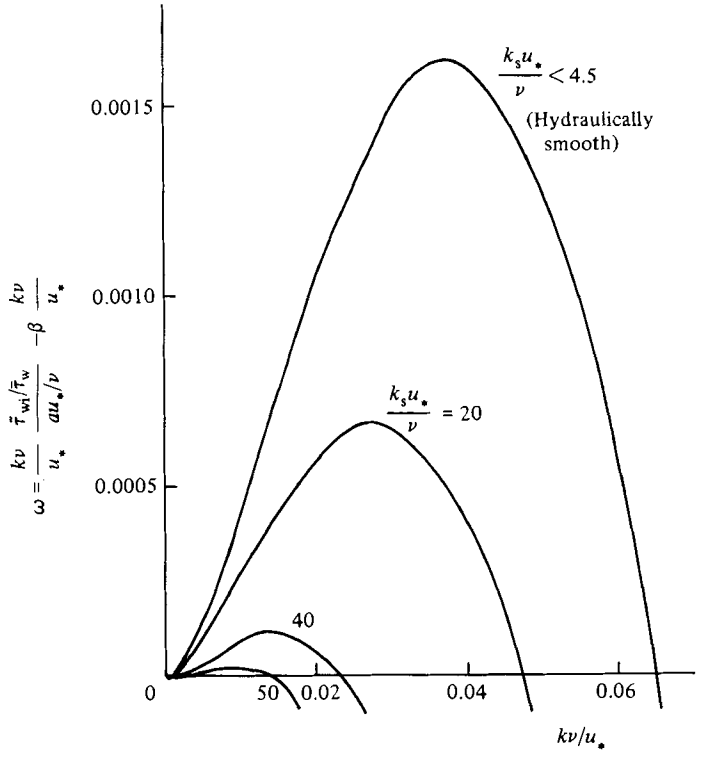

FIGURE 4. Growth rate for various values of $k_s u_*/\nu$; $\beta = 3.2$.

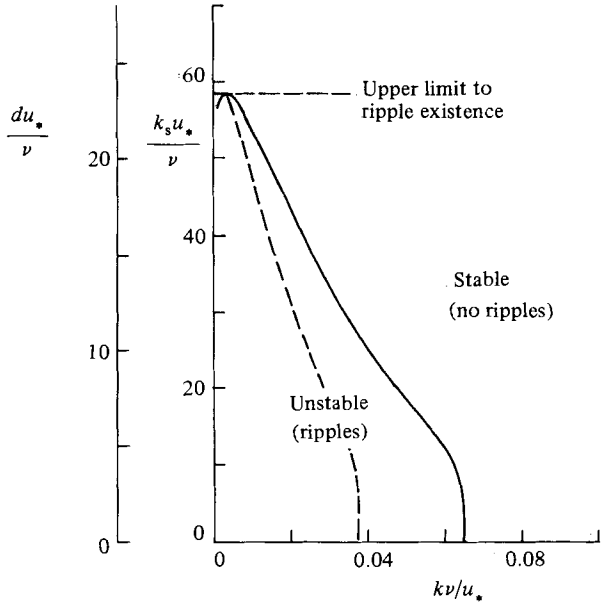

FIGURE 5. Stability limits to the formation of ripples; $\beta = 3.2$. The dashed curve corresponds to the fastest-growing wavenumber. k_s is converted to d by $k_s = 2.5\,d$.

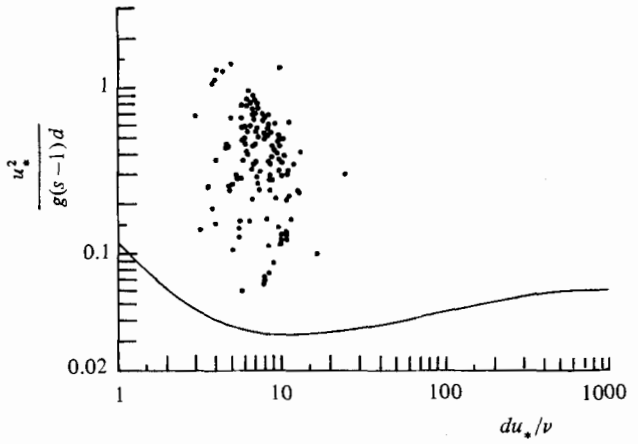

FIGURE 6. Plot of data for flows with ripple bed forms on Shields diagram (after Vanoni 1975).

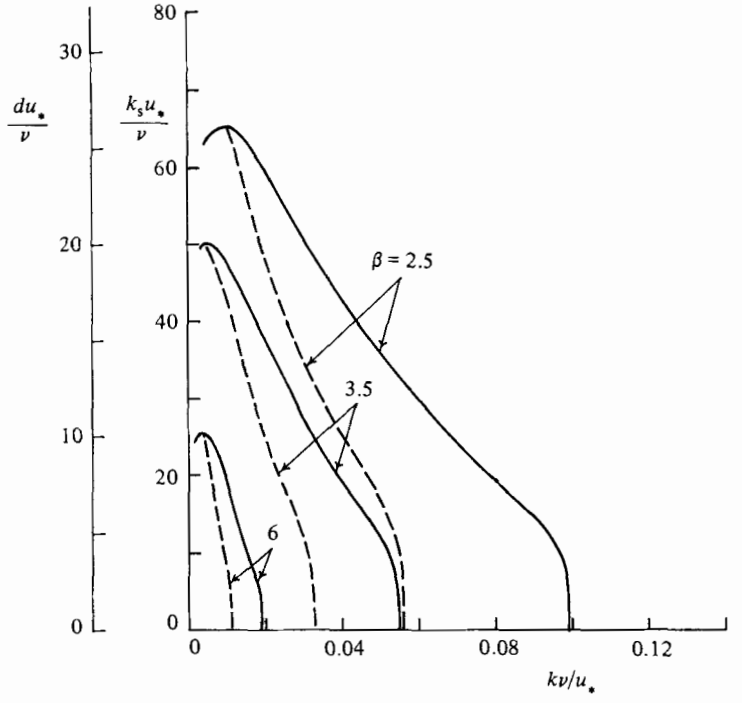

FIGURE 7. Effect of β on the stability limits to the formation of ripples. See caption of figure 3.

$k_s = 2.5\,d$ for the range of the Shields parameters du_*/ν and $u_*^2/g(s-1)d$ for which ripples are observed.

When converted to the grain Reynolds number using $k_s = 2.5\,d$, the upper limit to ripple existence, i.e. $k_s u_*/\nu = 58.5$, is found to be $du_*/\nu = 23$. This result is in remarkable agreement with the experimental information on ripple existence shown in figure 6, according to which no ripples have been observed for values of grain Reynolds number greater than approximately 25.

For the reported range of $\tan\phi$ quoted in Richards (1980), $0.32 < \tan\phi < 0.75$, which corresponds to the range $2.5 < \beta < 6$ (taking $c = 0.5$), the stability diagrams

are shown in figure 7, illustrating the effect of the parameter β upon the ripple instability. These diagrams show that the upper limit to ripple existence does not change significantly with the parameter β; in quantitative terms, above $du_*/\nu = 10$–26 no ripples will exist, which is again in good agreement with the experimental information in figure 6. As seen from figure 7, the limiting value of du_*/ν decreases with increasing β. This can be explained as follows. As has been pointed out in the preceding paragraph, we have zero 'gravity effect' when $\beta = 0$; the effect of gravity becomes more and more pronounced for increasing β. In the case of the gravity effect increasing with an increase in β, we need to have a larger wall shear stress to enable the erosion–transport–deposition process in ripple formation to keep continuing. As has been noted at the beginning of this section, the larger the amplitude of the wall shear stress, the smaller the roughness of the bed. This implies that the limiting value of $k_s u_*/\nu$ for ripple existence should decrease with increasing β.

As we should expect, the present model does not predict the existence of dunes. The formation of dunes depends on the flow depth. Furthermore, dunes are produced by suspended load perturbations. As the present theory does not take into consideration these latter effects, we should therefore not expect it to account for the existence of dunes.

On the other hand, for a stability theory to account for the transition from ripple to dune regimes, flow over fully developed ripples must be modelled; thus a nonlinear theory must be developed, including the effect of flow separation which occurs at the crests of mature ripples.

In figures 5 and 7, the dashed curves correspond to the fastest-growing wavenumber at which the growth rate ω attains a maximum positive value. This gives a preferred wavelength at which one would expect a disturbance to grow. From figure 5 the range of the fastest-growing wavenumber for varying du_*/ν is found to be $0.0035 < k\nu/u_* < 0.037$, with $k\nu/u_*$ increasing for decreasing du_*/ν. The latter range corresponds to the wavelength range $200 < Lu_*/\nu < 2000$, with Lu_*/ν increasing for increasing du_*/ν. This result has two immediate implications. First, in contrast with the earlier ideas (see e.g. Yalin 1972), the ripple length appears not to scale with the grain size d, but as a function of grain Reynolds number such that

$$\frac{Lu_*}{\nu} = f\left(\frac{du_*}{\nu}\right), \tag{24}$$

which is in complete agreement with Yalin's more recent (1977) study.† Secondly, the ripple length increases with increasing grain size, which is also in agreement with Yalin's (1977) study and also with Hayashi & Onishi's (1983) recent stability results.

However, the wavelength range $200 < Lu_*/\nu < 2000$ is an order of magnitude too small for observed ripples reported in Yalin (1977). Yalin, in this latter work, reports that during the development of ripples, their length can increase by a factor of two or so, and he points out that the development duration can be as long as several days; the values of the ripple lengths plotted in Yalin are those belonging to the fully developed ripples, the final lengths of which are expected to have been controlled by

† On dimensional grounds, Yalin (1977) actually gives $L/d = \phi(du_*/\nu)$. Referring to his earlier work (Yalin 1972), he notes that it was not possible to reveal the form of the function $\phi(du_*/\nu)$ by the available ripple data (which were scattered around the value 1000), and therefore there was no alternative but to represent $\phi(du_*/\nu)$ by the round value 1000; that is, $L/d \approx 1000$. However, in his more recent (1977) work, Yalin determines the functional form of $\phi(du_*/\nu)$ with the help of data obtained through a series of carefully designed experiments.

the separated flow over the fully developed wave. Since the present theory is a linear theory, and furthermore does not take into account the flow separation, and thus represents only the initial stage of ripple development, the preferred wavelengths obtained through the present theory should be considered as the initial (but not the final) lengths of ripples, and should therefore be small compared with those given in Yalin (1977). Fredsøe (1982) discusses in some detail the final dimensions and shape of ripples and dunes. He points out that the linear stability analyses are only able to predict whether bed forms develop or not, and can say almost nothing about the final dimensions and shape of the bed forms, supporting our argument above.

Finally, it should be pointed out that, although the initial preferred wavelength from figure 7 appears to be a function of the parameter β as well as du_*/ν, it should be a function of du_*/ν alone, since the parameter β itself should be expected to be a function of du_*/ν.

5. Conclusions

The results of the linear stability analysis developed to account for the formation of ripples show that an erodible bed will be unstable (and thus ripples will exist) when the grain Reynolds number is less than a certain value. The results appear to depend on the parameter β, the effect of the combined action of the gravity and the local bed slope upon the bed-load transport. It was found that, for $\beta = 3.2$ (an average value for β), no ripples will exist when the grain Reynolds number du_*/ν is above 23. It was also found that, for the range covered by β, ripples will not occur when the grain Reynolds number exceeds 10–26, depending on β. These results were found to compare remarkably well with observations.

Although the preferred initial wavelengths are found to be an order of magnitude too small for observed, fully developed ripples (owing to the fact that the present theory is linear, and furthermore does not take into account the flow separation at the crests of ripples), the present work implies that the ripple length non-dimensionalized by ν/u_* is a function of the grain Reynolds number du_*/ν, in contrast with the generally accepted assumption that the ripple length scales with grain size. The other implication of the present work is that the ripple length increases with grain size. These findings appear to be in qualitative agreement with recent observations.

REFERENCES

BAGNOLD, R. A. 1956 Flow of cohesionless grains in fluids. *Phil. Trans. R. Soc. Lond.* A **249**, 235.

BAGNOLD, R. A. 1973 The nature of saltation and of 'bed-load' transport in water. *Proc. R. Soc. Lond.* A **332**, 437.

BECCHI, I. 1983 Effects of sediment motion in river roughness. In *Proc. 2nd Intl Symp. on River Sedimentation. 11–16 Oct. 1983, Nanjing, China.* Water Resources and Electric Power Press.

CEBECI, T. & CHANG, K. C. 1978 Calculation of incompressible rough-wall boundary-layer flows. *AIAA J.* **16**, 730.

ENGELUND, F. & FREDSØE, J. 1982 Sediment ripples and dunes. *Ann. Rev. Fluid Mech.* **14**, 13.

ENGELUND, F. & HANSEN, E. 1967 *A Monograph on Sediment Transport in Alluvial Streams.* Teknisk Forlag, Copenhagen.

FOX, L. 1957 *The Numerical Solution of Two-Point Boundary Problems in Ordinary Differential Equations.* Clarendon.

FREDSØE, J. 1982 Shape and dimensions of ripples and dunes. In *Euromech 156: The Mechanics of Sediment Transport* (ed. B. M. Sumer & A. Muller). Balkema, Rotterdam.

HAYASHI, T. & ONISHI, M. 1983 Dominant wave numbers of ripples, dunes and antidunes on alluvial river beds. In *Proc. 2nd Intl Symp. on River Sedimentation, 11–16 Oct. 1983, Nanjing, China.* Water Resources and Electric Power Press.

KENNEDY, J. F. 1980 Bed forms in alluvial streams: some views on current understanding and identification of unresolved problems. In *Application of Stochastic Processes in Sediment Transport* (ed. H. W. Shen & H. Kikkawa). Water Resources Publications, Colorado.

LOYD, R. J., MOFFAT, R. J. & KAYS, W. M. 1970 The turbulent boundary layer on a porous plate: an experimental study of the fluid dynamics with strong favourable pressure gradients and blowing. *Dept Mech. Engng Stanford Univ. Rep.* HMT-13.

MANTZ, P. A. 1978 Bed forms produced by fine, cohesionless, granular and flakey sediments under subcritical water flows. *Sedimentology* **25**, 83.

MONIN, A. S. & YAGLOM, A. M. 1971 *Statistical Fluid Mechanics: Mechanics of Turbulence*, vol. 1. MIT Press.

REYNOLDS, A. J. 1976 A decade's investigation of the stability of erodible stream beds. *Nord. Hydrol.* **7**, 161.

RICHARDS, K. J. 1980 The formation of ripples and dunes on an erodible bed. *J. Fluid. Mech.* **99**, 597.

ROTTA, J. C. 1962 Turbulent boundary layers in incompressible flow. *Prog. Aerospace Sci.* **2**, 1.

SUMER, B. M. & BAKIOGLU, M. 1983 Instability of erodible bed: ripple formation. In *Proc. 2nd Intl Symp. on River Sedimentation, 11–16 Oct. 1983, Nanjing, China.* Water Resources and Electric Power Press.

SUMER, B. M., BAKIOGLU, M. & BULUTOGLU, A. 1982 Ripple formation on a bed of fine, cohesionless, granular sediment. In *Euromech 156: The Mechanics of Sediment Transport* (ed. B. M. Sumer & A. Muller). Balkema, Rotterdam.

THORSNESS, C. B., MORRISROE, P. E. & HANRATTY, T. J. 1978 A comparison of linear theory with measurements of the variation of shear stress along a solid wave. *Chem. Engng Sci.* **33**, 579.

VANONI, V. 1975 Factors determining bed forms of alluvial streams. Closure. *J. Hydraul. Div. ASCE* **101** (HY11), 1435.

YALIN, M. S. 1972 *Mechanics of Sediment Transport.* Pergamon.

YALIN, M. S. 1977 On the determination of ripple length. *J. Hydraul. Div. ASCE* **103** (HY4), 439.

ZILKER, D. P., COOK, G. W. & HANRATTY, T. J. 1977 Influence of the amplitude of a solid wavy wall on a turbulent flow. Part 1. Non-separated flows. *J. Fluid Mech.* **82**, 29.